

AD-A048 364

AIR FORCE INST OF TECH WRIGHT-PATTERSON AFB OHIO SCH--ETC F/G 11/4
A GENERAL STUDY OF HYBRID COMPOSITE LAMINATES.(U)

DEC 77 G D BROOKS

UNCLASSIFIED

AFIT/GAE/AA/77D-2

NL

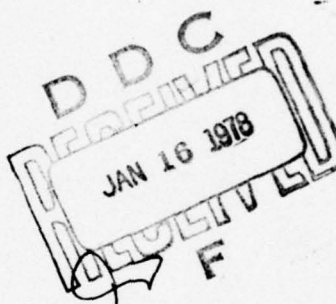
1 OF 1
AD
A048364

11
11



END
DATE
FILMED
2- 78
DDC

AFIT/GAE/AA/77D-2



A GENERAL STUDY OF
HYBRID COMPOSITE LAMINATES

THESIS

AFIT/GAE/AA/77D-2

George Brooks
Capt USAF

Approved for public release; distribution unlimited.

A GENERAL STUDY OF
HYBRID COMPOSITE LAMINATES

THESIS

Presented to the Faculty of the School of Engineering
of the Air Force Institute of Technology
Air University
in Partial Fulfillment of the
Requirements for the Degree of
Master of Science

by

George D. Brooks, B.S.M.E.

Captain

USAF

Graduate Aeronautical Engineering

December 1977

ACCESSION for	
NTIS	White Section <input checked="" type="checkbox"/>
DDC	Buff Section <input type="checkbox"/>
UNANNOUNCED	<input type="checkbox"/>
JUSTIFICATION	
BY	
DISTRIBUTION/AVAILABILITY CODES	
Dist	SPECIAL
A	

Approved for public release; distribution unlimited.

Preface

Hybrid composite laminates are a fairly recent innovation into the aircraft industry. These hybrids are designed to have certain characteristics of strength not found in homogeneous composite laminates. Very little work has been documented to assure that these hybrids follow classical laminated plate theory and the corresponding assumptions. I have performed a general study of hybrid composite laminates which includes three dimensional stress analysis, thermal residual stress effects, effects of hybridization, and analysis of two existing hybrid laminates.

I express my appreciation especially to Dr. Anthony N. Palazotto for his timely advice, encouragement, and instruction that aided immensely in completion of this report. I thank Dr. James Whitney and Mr. Marvin Knight of the Air Force Materials Laboratory for their support and assistance during this study. The patience of my family during this study is greatly appreciated.

George D. Brooks

Contents

	<u>Page</u>
Preface	ii
List of Figures	iv
List of Tables	v
List of Symbols	vi
Abstract	viii
 I. Introduction	 1
Background	1
Purpose	3
 II. Theory	 7
Laminated Plate Relationships	7
Free Edge Effect	14
Apparent Modulus of Elasticity	18
 III. Results	 22
Verification of Computer Program	22
Effects of Addition of Hybrid Material	24
A. Eight Ply Specimen	24
B. Twelve Ply Specimen	32
Experimental Results with 48 ply Specimen	35
Application of Tsai-Hill Failure Criteria to Hybrid Composites	39
 IV. Conclusions	 42
 Bibliography	 44
 Appendix A: Transverse Shear Deformation	 47
 Appendix B: Physical Description of Specimens	 50
 Vita	 53

List of Figures

<u>Figure</u>	<u>Page</u>
1. Illustration of 80-20 Hybrid Composite Material	5
2. Load Axes Relative to Material Property Axes	8
3. Cross Section of Laminate	8
4. Mechanism for Computation of τ_{xz}^k	15
5. Mechanism for Computation of τ_{yz}^k and σ_z^k	15
6. Distribution of Interlaminar Normal Stress versus y	17
7. Distribution of σ_x in 8 ply Laminate-Tensile Load	26
8. Distribution of σ_y in 8 ply Laminate-Tensile Load	26
9. Distribution of σ_z in 8 ply Laminate-Tensile Load	27
10. Distribution of τ_{xy} in 8 ply Laminate-Tensile Load	27
11. Distribution of τ_{yz} in 8 ply Laminate-Tensile Load	28
12. Distribution of τ_{xz} in 8 ply Laminate-Tensile Load	28
13. Distribution of σ_x in 8 ply Laminate-Flexure Load	30
14. Distribution of σ_y in 8 ply Laminate-Flexure Load	30
15. Distribution of σ_z in 8 ply Laminate-Flexure Load	31
16. Distribution of τ_{yz} in 8 ply Laminate-Flexure Load	31
17. Experimental Load-Displacement Curves for 48 ply Specimens Under Tensile Load	36
18. Experimental Load-Deflection Curves for 48 ply Specimens Under Flexure Load	37
19. Section of a Flexure Loaded Beam	47

List of Tables

<u>Table</u>	<u>Page</u>
I. Maximum Value of Interlaminar Normal Stress, σ_z	25
II. Effective Tensile Modulus of Elasticity, \bar{E}_x	29
III. Effective Flexure Modulus of Elasticity	33
IV. Deflection of Beam Specimen With and Without Shear Load at Quarter Points	34
V. Modulus of Elasticity	38
VI. Predicted Loads at First Lamina Failure	40

List of Symbols

b	half dimension of specimen in the y-direction, in.
E_{11}, E_{22}	modulus of a unidirectional composite in the longitudinal and transverse directions of the fiber axes, respectively, lb/in ² .
\bar{E}_{11}	apparent tensile/flexure modulus of a composite beam in the x-direction, lb/in ² .
E_x^k	modulus in the x-direction of the kth layer of a laminated composite, lb/in ² .
G_{12}	shear modulus of a unidirectional composite in the 1-2 plane, lb/in ² .
h	thickness of specimen, in.
I	beam area moment of inertia, in ² .
I^k	area moment of inertia of kth layer of a laminated beam with respect to the middle plane, in ² .
k	shear distribution parameter
M	moment applied to beam, in-lb.
M_x, M_y, M_{xy}^T	bending and twisting moments per unit length of plate surface, in-lb/in.
M_x^T, M_y^T, M_{xy}^T	bending and twisting moments per unit length of plate surface caused by the thermal residual stresses, in-lb/in.
M_z	free edge effect moment equivalent to $\sigma_z h$, lb-in.
N_x, N_y, N_{xy}	force components per unit length of plate surface, lb/in.
N_x^T, N_y^T, N_{xy}^T	force components per unit length of plate surface by residual thermal stresses, lb/in.
P	total flexure load applied, lb.
Q_{ij}, \bar{Q}_{ij}	terms of the composite laminate stiffness matrix in the material and load axes, respectively, lb/in ² .
Q_x	shear resultant per unit length of plate surface, lb/in.
u, v, w	displacements of a specimen in the x, y, z directions, respectively, in.

s_{11}	compliance matrix component in the longitudinal material axes direction
t	lamina thickness, in.
x, y, z	load axes of a specimen
X, Y, S	ultimate strengths in the longitudinal, transverse, shear material directions, respectively, lb/in ² .
$1, 2, 3$	material property axes of a specimen
α_1, α_2	thermal coefficients of expansion in the material axes directions, in/in - °F.
$\alpha_x, \alpha_y, \alpha_{xy}$	thermal coefficients of expansion in the load axes directions, in/in - °F.
Δl	change of length of a specimen, in.
ΔT	change in temperature, °F.
$\epsilon_1, \epsilon_2, \epsilon_3$	strains in the material axes, in/in.
$\epsilon_x, \epsilon_y, \epsilon_{xy}$	strains in the load axes, in/in.
$\epsilon_x^0, \epsilon_y^0, \epsilon_{xy}^0$	strains of the middle surface of a plate, in/in.
ν_{12}, ν_{21}	Poisson's ratio in the longitudinal and transverse material directions, respectively.
k_x, k_y, k_{xy}	curvatures of a plate, 1/in.
$\sigma_1, \sigma_2, \sigma_3$	normal stress in the material axes, lb/in ² .
$\tau_x, \tau_y, \tau_{xy}$	normal stress in the load axes, lb/in ² .
$\tau_{xy}, \tau_{xz}, \tau_{yz}$	shear stress in the load axis, lb/in ² .
ψ, ψ^1	displacement functions.

Abstract

This thesis is a general study of hybrid composite laminates that includes application of a three dimensional stress analysis approximation technique based on equilibrium considerations and free edge effects. Thermal residual stresses and effects of replacing lamina in a composite laminate with lamina composed of hybrid material were investigated. Two types of 48 ply hybrid composite laminates were tested under tensile and flexure loading. Results achieved experimentally for the moduli of elasticity were compared with values predicted by laminated plate theory and laminated beam theory. Thermal residual stresses proved to be significant and worthy of due consideration in stress analysis of test specimens. Hybridization, as studied, appeared to have little effect on the overall properties of a laminate. Hybrid composite laminates obey classical laminate theory and can, in certain ply configurations, develop considerable free edge effect stresses.

A GENERAL STUDY
OF
HYBRID COMPOSITE LAMINATES

I. Introduction

Background

In recent years, hybrid composite laminates, the result of mixing different kinds of fibers, i.e., glass with graphite fibers, either in the same matrix or as different lamina within a laminate, have made a successful appearance within the aerospace industry due to their economy and impact resistance characteristics. Yet, little work has been documented to assure that these hybrids follow the classical laminated plate theory and the assumption of two dimensionality. This becomes important since evaluation of material strength properties are commonly arrived at through testing of scaled down specimens. Thus, it is justified to explore further the use of classical theory with primary attention given to hybrid composites.

Although laminated plate theory has been used for many years in analysis of composite laminates [1,6], previous studies show that caution must be used when testing for material property characteristics for a specific material [14,25]. Several important aspects should be considered thoroughly in design of composites. Among these are shear coupling distortion in bending modes, free edge effects as pertained to the lamina failure in addition to possible delamination, and residual thermal stresses induced by the curing process. These aspects will be discussed separately.

Whitney has discussed the phenomenon of shear coupling distortion during flexure tests and the resulting effect on the measured modulus of elasticity. Wide use of flexure tests has been the result of end constraint problems associated with tensile testing. Whitney, et al [23], demonstrated the inadequacy of the flexure test since the bending stiffness is a function of ply stacking sequence. This work [23] clearly illustrated the limitation of data obtained by flexure testing. Under conditions where a laminate is designed for a certain load, characteristics obtained by similar loading of a test specimen may be more accurate. However, use of material characteristics obtained by flexure tests may not be adequate for use in tensile loading environments or vice versa.

The aspect of free edge stress effect, defined graphically in Figures 4 and 5, and the corresponding limitations of two-dimensional laminate theory have been investigated by several sources [10,13,14]. These studies have shown the existence of significant interlaminar shear and normal forces which are considered insignificant by classical laminate plate theory. Puppo and Eversen [14] showed that properties developed by two different test specimen geometries, one with free edges and one without free edges, might have significant differences due to the free edge effect of the interlaminar shear forces. Finite difference studies by Pipes and Pagano [13] have shown that these free edge stresses are generally significant only in a region measured inward from a free edge over a width equal to the thickness dimension of the laminated plate. Pipes and Pagano also demonstrated that interior regions outside of

these restricted areas can be treated adequately by laminated plate theory. One can readily see that the width to thickness ratio of a test specimen would be a critical value in manufacturing test specimens. The narrow specimens would have a large percentage of area effected by free edge stresses. Analytical solutions by Tang [16] showed that the normal stresses, σ_z , can be from 5 to 30 percent of the applied load for uniaxially loaded specimens. The magnitude of these stresses may approach the ultimate strength of the material.

Composite materials are limited by the minimum strength of the matrix material and/or the bond between fibers and matrix material. Interlaminar shear stresses τ_{yz} , and τ_{xz} , or the normal stress, σ_z , that exceed this minimum strength of the composite can cause a failure mode not heretofore predicted by laminate theory [10] (see Figure 2). Thus, free edge effect stresses have lately become a major concern because of this failure potential.

The aspect of thermally induced stresses in a two-dimensional sense is treated by laminate plate theory. Unless the test is performed in an environmentally controlled chamber at cure temperature, the normal test specimen is exposed to stresses brought about by the high temperatures used in the curing process for composite materials. These temperatures generally are 300°-350°F. Therefore, a test specimen at 70°F is subjected to thermally induced stresses that should be considered in test results. Wang and Crossman [20] have used a finite element technique to study the distribution of thermally induced free edge effect stresses not considered by classical laminate theory and have predicted free edge stresses of considerable magnitude for certain laminate configurations. The resultant of stresses caused by the three aspects discussed may cause

failure in laminates.

Purpose

This thesis study has a twofold purpose. Values for the tensile modulus of elasticity predicted by the composite laminate transformation equations and likewise, values for an apparent flexure modulus of elasticity will be compared with values obtained experimentally. Using theory developed by Whitney [23], the shear coupling effect will be considered also. Two panels of 48 ply symmetric hybrid composite laminates were available. The microstructure of the hybrid lamina is composed of 80 percent by volume of graphite fibers in epoxy resin and 20 percent by volume of glass fibers in epoxy resin. The glass fibers are laid in ribbon fashion. See Figure 1. The panels differ in that panel #1 contains several 0° plies of glass fiber/epoxy layers and in panel #2 these 0° oriented plies are composed of the 80-20 hybrid material.

The secondary goal of this study is to develop a three dimensional stress approximation technique that will predict values for the maximum edge effect stresses in hybrid laminates. This work is based on equilibrium equation solutions for finite sized elements [12]. The method assumes the interlaminar normal stress distribution indicated by Pipes and Pagano [13], and their approximate distribution will be used for calculation of the normal stress, σ_z . This distribution is assumed valid for uniaxial, bending, and thermal stresses. Several techniques have been used recently to obtain approximations incorporating free edge stresses. These techniques include finite element solutions by Wang and Crossman [20] and perturbation theory applications by Hsu and Herakovitch [5]. Work by Wang and Crossman assumed a different thermal stress distribution from that of Pipes and Pagano. The results

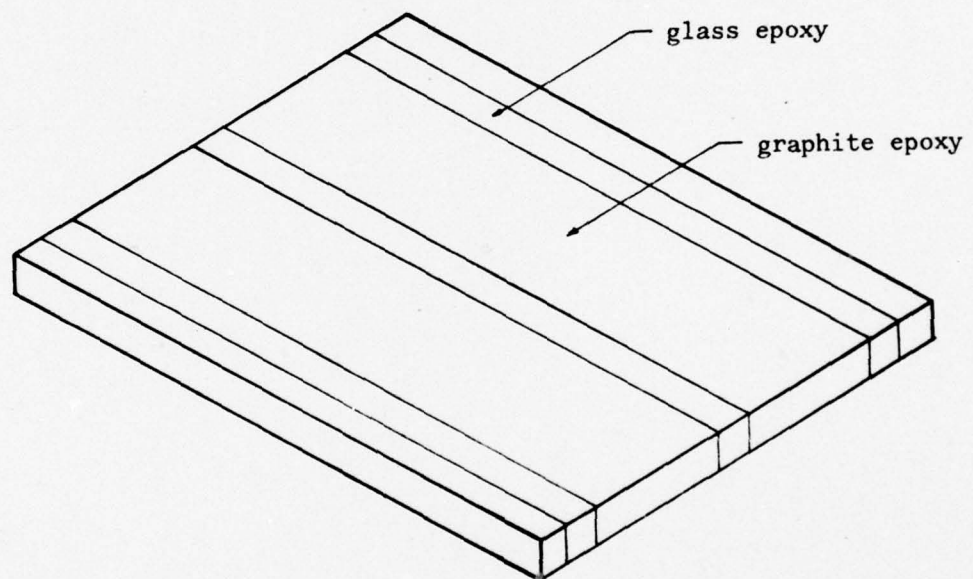


Fig. 1. Illustration of 80-20 Hybrid Composite Material Lamina

of this thesis study will be compared to the results obtained by Wang and Crossman by using their ply geometries acting under a $\Delta T = 1^{\circ}\text{F}$.

This study also explores the application of a failure criteria to stress fields predicted analytically. There are several failure criteria models available, i.e., maximum stress, maximum strain, Tsai-Hill theory [6]. The maximum stress theory predicts fracture if stresses in the principal material directions exceed the respective ultimate strengths in those directions. The maximum strain theory is similar in that strains are limited rather than stresses. There is no interaction between modes of failure in these criteria. Each treats the respective principal direction as a subcriteria. Hill's approach [4] is based on a Von Mises criterion. This work was modified by Tsai [18] and consequently became known as the Tsai-Hill theory. The resulting failure theory utilizes the principal direction ultimate strengths, but there is interaction between modes of failure. This interaction makes the theory more applicable to composite laminates. The Tsai-Wu theory incorporates the fact that composites generally have different strengths under tensile and compressive loading. Results of previous laboratory tests [8] and results of the laboratory tests of this study will be used to determine the accuracy as predicted by the Tsai-Hill failure theory.

This thesis should give a better understanding of the applicability of classical laminate theory to hybrid composite laminates as well as an approximation of the maximum stresses that may be encountered in a particular composite laminate design.

II. Theory

Laminated Plate Relationships

The intent of this section is to collect some of the classical laminated plate relationships for background [23] and develop the theory that is applied specifically in this thesis study [10, 13].

Figure 2 indicates the material property (1,2,3) and the load (x,y,z) axes directions. For any particular ply, the lamina stiffness matrix for an orthotropic material relative to the material axes is:

$$\begin{Bmatrix} \sigma_1 \\ \sigma_2 \\ \sigma_3 \end{Bmatrix}^k = \begin{bmatrix} Q_{11} & Q_{12} & Q_{16} \\ Q_{12} & Q_{22} & Q_{26} \\ Q_{16} & Q_{26} & Q_{66} \end{bmatrix}^k \begin{Bmatrix} \epsilon_1 \\ \epsilon_2 \\ \epsilon_{12} \end{Bmatrix}^k \quad (1)$$

where the components of the stiffness matrix are:

$$\begin{aligned} Q_{11} &= E_{11}/(1-\nu_{12}\nu_{21}) \\ Q_{22} &= E_{22}/(1-\nu_{12}\nu_{21}) \\ Q_{12} &= \nu_{12}E_{11}/(1-\nu_{12}\nu_{21}) = \nu_{12}E_{22}/(1-\nu_{12}\nu_{21}) \\ Q_{66} &= G_{12} \\ Q_{16} &= Q_{26} = 0 \end{aligned} \quad (2)$$

For a lamina, with its material property axes oriented at some angle, θ , to the loading axes, the stiffness matrix is given by:

$$\begin{Bmatrix} \sigma_x \\ \sigma_y \\ \sigma_{xy} \end{Bmatrix}^k = \begin{bmatrix} \bar{Q}_{11} & \bar{Q}_{12} & \bar{Q}_{16} \\ \bar{Q}_{16} & \bar{Q}_{22} & \bar{Q}_{26} \\ \bar{Q}_{16} & \bar{Q}_{26} & \bar{Q}_{66} \end{bmatrix}^k \begin{Bmatrix} \epsilon_x \\ \epsilon_y \\ \epsilon_{xy} \end{Bmatrix}^k \quad (3)$$

where

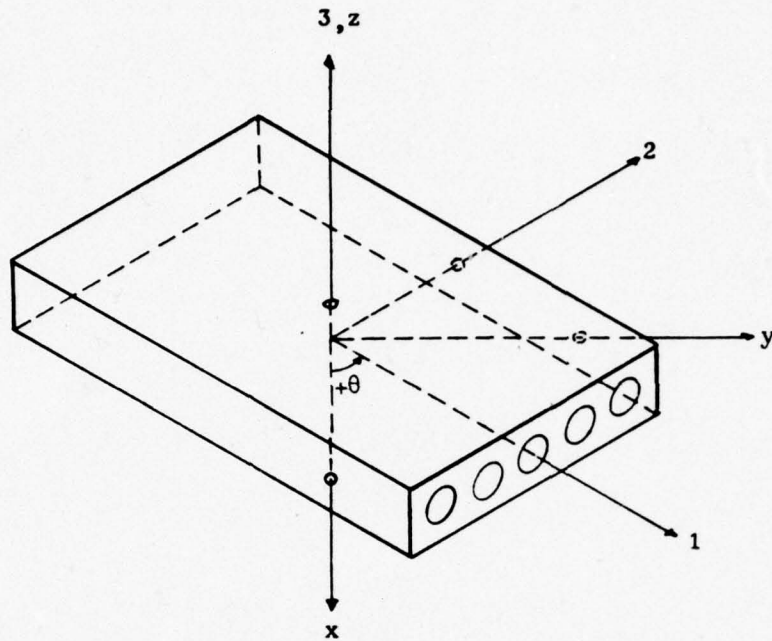


Fig. 2. Load Axes Relative to Material Property Axes

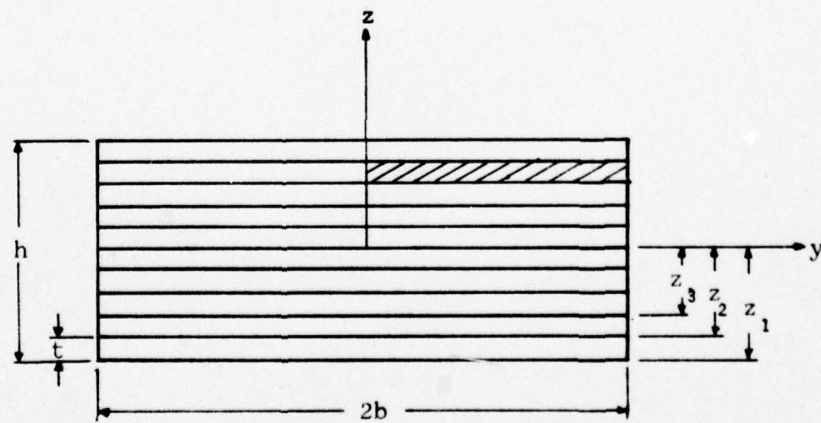


Fig. 3. Cross Section of Laminate

$$\begin{aligned}
\bar{Q}_{11} &= Q_{11} \cos^4 \theta + 2(Q_{12} + 2Q_{66}) \sin^2 \theta \cos^2 \theta + Q_{22} \sin^4 \theta \\
\bar{Q}_{22} &= Q_{11} \sin^4 \theta + 2(Q_{12} + 2Q_{66}) \sin^2 \theta \cos^2 \theta + Q_{22} \cos^4 \theta \\
\bar{Q}_{12} &= (Q_{11} + Q_{22} - 4Q_{66}) \sin^2 \theta \cos^2 \theta + Q_{12} (\sin^4 \theta + \cos^4 \theta) \\
\bar{Q}_{66} &= (Q_{11} + Q_{22} - 2Q_{12} - 2Q_{66}) \sin^2 \theta \cos^2 \theta + Q_{66} (\sin^4 \theta + \cos^4 \theta) \\
\bar{Q}_{16} &= (Q_{11} - Q_{12} - 2Q_{66}) \sin \theta \cos^3 \theta + (Q_{12} - Q_{22} + 2Q_{66}) \sin^3 \theta \cos \theta \\
\bar{Q}_{26} &= (Q_{11} - Q_{12} - 2Q_{66}) \sin^3 \theta \cos \theta + (Q_{12} + 2Q_{66}) \sin \theta \cos^3 \theta
\end{aligned} \tag{4}$$

The strain components are

$$\begin{Bmatrix} \epsilon_x \\ \epsilon_y \\ \epsilon_{xy} \end{Bmatrix} = \begin{Bmatrix} \epsilon_x^0 \\ \epsilon_y^0 \\ \epsilon_{xy}^0 \end{Bmatrix} + z \begin{Bmatrix} k_x \\ k_y \\ k_{xy} \end{Bmatrix} - \begin{Bmatrix} \epsilon_x^T \\ \epsilon_y^T \\ \epsilon_{xy}^T \end{Bmatrix} \tag{5}$$

where

$$\begin{Bmatrix} \epsilon_x^0 \\ \epsilon_y^0 \\ \epsilon_{xy}^0 \end{Bmatrix} = \begin{Bmatrix} \partial u / \partial x \\ \partial v / \partial y \\ \frac{\partial u}{\partial y} + \frac{\partial v}{\partial x} \end{Bmatrix} \tag{6}$$

and

$$\begin{Bmatrix} k_x \\ k_y \\ k_{xy} \end{Bmatrix} = \begin{Bmatrix} -\frac{\partial^2 \omega}{\partial x^2} \\ -\frac{\partial^2 \omega}{\partial y^2} \\ -2 \frac{\partial^2 \omega}{\partial x \partial y} \end{Bmatrix} \tag{7}$$

and

$$\begin{Bmatrix} \epsilon_x^T \\ \epsilon_y^T \\ \epsilon_{xy}^T \end{Bmatrix} = \begin{Bmatrix} \alpha_x \\ \alpha_y \\ \alpha_{xy} \end{Bmatrix} \Delta T \tag{8}$$

where α_i are the thermal coefficients of expansion in the load axis system.

The laminate constitutive relationship, assuming $\Delta T = 0$, is given by

$$\begin{Bmatrix} N \\ M \end{Bmatrix} = \begin{vmatrix} A & B \\ B & D \end{vmatrix} \begin{Bmatrix} \epsilon^0 \\ \kappa \end{Bmatrix} \quad (9)$$

where

$$N_i = \int_{-h/2}^{h/2} \sigma_i dz \quad (10)$$

$$M_i = \int_{-h/2}^{h/2} \sigma_i z dz$$

and

$$A_{ij} = \int_{-h/2}^{h/2} \bar{Q}_{ij} dz$$

$$B_{ij} = \int_{-h/2}^{h/2} \bar{Q}_{ij} z dz \quad (11)$$

$$D_{ij} = \int_{-h/2}^{h/2} \bar{Q}_{ij} z^2 dz$$

When the laminate is symmetric, i.e., for each angle ply lamina above the midplane there is a similarly oriented ply located the same distance

below the midplane, then Equation (11) becomes:

$$B_{ij} = 0$$

and Equation (9) becomes:

$$\begin{Bmatrix} N \\ - \\ M \end{Bmatrix} = \begin{bmatrix} A & 0 \\ 0 & D \end{bmatrix} \begin{Bmatrix} \epsilon^0 \\ - \\ k \end{Bmatrix} \quad (12)$$

and the axial and moment loads are uncoupled.

Equation (12) written in expanded form is

$$\begin{Bmatrix} N_x \\ N_y \\ N_{xy} \end{Bmatrix} = [A] \begin{Bmatrix} \epsilon_x^0 \\ \epsilon_y^0 \\ \epsilon_{xy}^0 \end{Bmatrix} \quad (13)$$

and

$$\begin{Bmatrix} M_x \\ M_y \\ M_{xy} \end{Bmatrix} = [D] \begin{Bmatrix} k_x \\ k_y \\ k_{xy} \end{Bmatrix} \quad (14)$$

When thermal expansion strain is included, the stress can then be evaluated from:

$$\begin{Bmatrix} \sigma_x \\ \sigma_y \\ \sigma_{xy} \end{Bmatrix}^k = [\bar{Q}_{ij}]^k \begin{Bmatrix} \epsilon_x - \alpha_x \Delta T \\ \epsilon_y - \alpha_y \Delta T \\ \epsilon_{xy} - \alpha_{xy} \Delta T \end{Bmatrix}^k \quad (15)$$

Equations (13) and (14) become

$$\begin{Bmatrix} N_x \\ N_y \\ N_{xy} \end{Bmatrix} = [A] \begin{Bmatrix} \epsilon_x^0 \\ \epsilon_y^0 \\ \epsilon_{xy}^0 \end{Bmatrix} - \begin{Bmatrix} N_x^T \\ N_y^T \\ N_{xy}^T \end{Bmatrix} \quad (16)$$

where

$$\begin{Bmatrix} N_x^T \\ N_y^T \\ N_{xy}^T \end{Bmatrix} = \int_{-h/2}^{h/2} [\bar{Q}_{ij}]^k \begin{Bmatrix} \alpha_x \\ \alpha_y \\ \alpha_{xy} \end{Bmatrix}^k \Delta T dz \quad (17)$$

and

$$\begin{Bmatrix} M_x \\ M_y \\ M_{xy} \end{Bmatrix} = [D] \begin{Bmatrix} k_x \\ k_y \\ k_{xy} \end{Bmatrix} - \begin{Bmatrix} M_x^T \\ M_y^T \\ M_{xy}^T \end{Bmatrix} \quad (18)$$

where

$$\begin{Bmatrix} M_x^T \\ M_y^T \\ M_{xy}^T \end{Bmatrix} = \int_{-h/2}^{h/2} [\bar{Q}_{ij}]^k \begin{Bmatrix} \alpha_x \\ \alpha_y \\ \alpha_{xy} \end{Bmatrix}^k \Delta T z dz \quad (19)$$

For symmetric laminates, $\{M_i^T\} = 0$.

For given loads the strains may be found by taking the inverse relationships of Equations (16) and (18).

$$\begin{Bmatrix} \epsilon_x^0 \\ \epsilon_y^0 \\ \epsilon_{xy}^0 \end{Bmatrix} = [A]^{-1} \begin{Bmatrix} N_x + N_x^T \\ N_y + N_y^T \\ N_{xy} + N_{xy}^T \end{Bmatrix} \quad (20)$$

and

$$\begin{Bmatrix} k_x \\ k_y \\ k_{xy} \end{Bmatrix} = [D]^{-1} \begin{Bmatrix} M_x + M_x^T \\ M_y + M_y^T \\ M_{xy} + M_{xy}^T \end{Bmatrix} \quad (21)$$

If one assumes that plane sections remain plane in bending and that the displacement is constant across the face during axial loading, the total strain experienced by a specimen under combined loading of N_x , M_x , and a ΔT would be

$$\begin{Bmatrix} \epsilon_x \\ \epsilon_y \\ \epsilon_{xy} \end{Bmatrix} = [A]^{-1} \begin{Bmatrix} N_x + N_x^T \\ N_y^T \\ N_{xy}^T \end{Bmatrix} + z[D]^{-1} \begin{Bmatrix} M_x + M_x^T \\ M_y^T \\ M_{xy}^T \end{Bmatrix} \quad (22)$$

Combined loading is not used in this study so Equation (22) for axial load, N_x , can be written as

$$\begin{Bmatrix} \epsilon_x \\ \epsilon_y \\ \epsilon_{xy} \end{Bmatrix} = [A]^{-1} \begin{Bmatrix} N_x + N_x^T \\ N_y^T \\ N_{xy}^T \end{Bmatrix} \quad (23)$$

and for a bending moment, M_x ,

$$\begin{Bmatrix} \epsilon_x \\ \epsilon_y \\ \epsilon_{xy} \end{Bmatrix} = [A]^{-1} \begin{Bmatrix} N_x^T \\ N_y^T \\ N_{xy}^T \end{Bmatrix} + z[D]^{-1} \begin{Bmatrix} M_x \end{Bmatrix} \quad (24)$$

From Equation (3), the two dimensional stresses due to axial load may be found from the following expression for any kth lamina

$$\begin{Bmatrix} \sigma_x \\ \sigma_y \\ \sigma_{xy} \end{Bmatrix}^k = [\bar{Q}_{ij}]^k [A]^{-1} \begin{Bmatrix} N_x + N_x^T \\ N_y^T \\ N_{xy}^T \end{Bmatrix} \quad (25)$$

and for moment loads by

$$\begin{Bmatrix} \sigma_x \\ \sigma_y \\ \sigma_{xy} \end{Bmatrix}^k = [\bar{Q}_{ij}]^k z[D]^{-1} \begin{Bmatrix} M_x \end{Bmatrix} + [A]^{-1} \begin{Bmatrix} N_x^T \\ N_y^T \\ N_{xy}^T \end{Bmatrix} \quad (26)$$

Free Edge Effect

Interlaminar stresses have been displayed in equation form in [12]. Free body diagrams [Figures 4 and 5] are used to illustrate the shear stress and normal stress mechanisms caused by the free edge effect. (The reader should realize that this analysis is an attempt at eliminating the inconsistency due to the necessity of zero edge stress in laminated plate theory) For a section of length with unit dimension, a summation of moments about the z axis yields the following:

$$\Sigma M_z = 0$$

$$\tau_{xy}^k(t)(2b)(1) + \tau_{xz}^k(1)(h)(2b-h) - \tau_{xz}^{k-1}(1)(h)(2b-h) = 0 \quad (27a)$$

$$\tau_{xz}^k = -\tau_{xy}^k \frac{2tb}{h(2b-h)} + \tau_{xz}^{k-1} \quad (27b)$$

For the outer lamina $\tau_{xz}^{k-1} = 0$.

Figure 5 is a representation of the shaded cross section of Figure 3. The interlaminar shear stress can be found from a summation of forces in the y-direction acting on a unit depth.

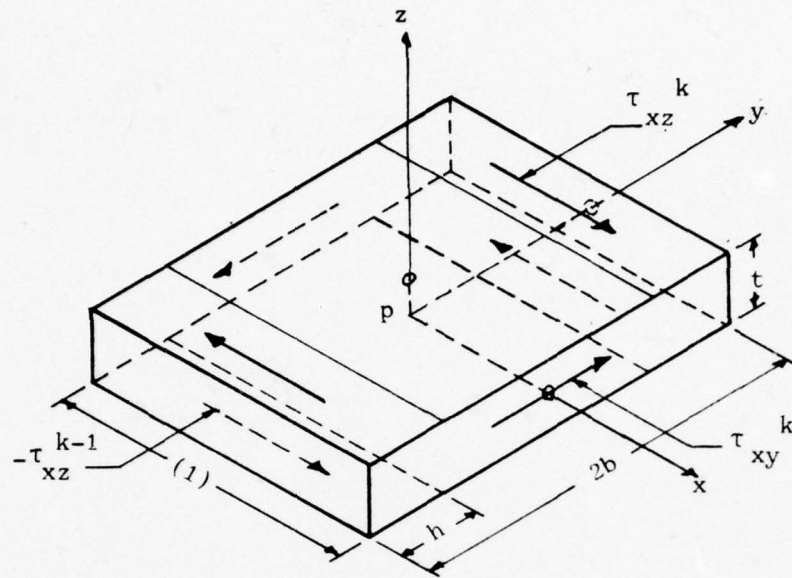


Fig. 4. Mechanism for Computation of τ_{xz}^k

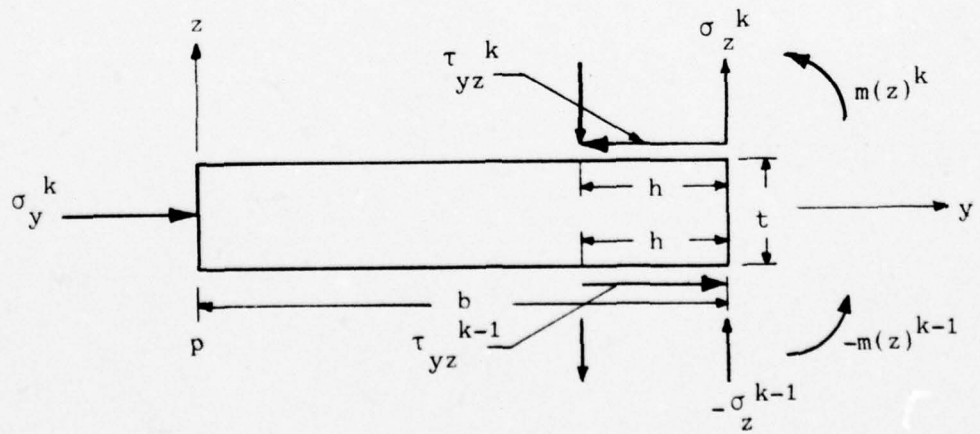


Fig. 5. Mechanism for Computation of τ_{yz}^k and σ_z^k

$$\Sigma F_y = 0$$

$$\sigma_y^k(1)(t) + \tau_{yz}^k(1)(h) - \tau_{yz}^{k-1}(1)(h) = 0$$

$$\tau_{yz}^k = -\sigma_y^k(t/h) + \tau_{yz}^{k-1} \quad (27)$$

Pipes and Pagano [11] concluded that the interlaminar normal stress distribution might be approximated by a function displayed in Figure 6.

From Figure 5, the $\sigma_z^k h$ couple is equivalent to the free edge moment $M_{(z)}^k$. The equation for σ_z^k is developed from Figure 6 as follows:

$$\Sigma F_z = 0$$

$$[(\sigma_z + \sigma_z^1)(\frac{1}{2})(1/3) - \sigma_z^1(1/3) - \sigma_z^1(2/3)](2b) = 0$$

$$\sigma_z^1 = \sigma_z/5 \quad (28)$$

$$\Sigma M_A = 0$$

$$(\sigma_z + \sigma_z^1)(\frac{1}{2})(1/3)(2b)(2/3 + 2/3(1/3))(2b)$$

$$- \sigma_z^1(1/3)(2b)(2/3 + \frac{1}{2}(1/3))(2b)$$

$$- \sigma_z^1(2/3)(2b)(1/3)(2b) = \frac{M_{(z)}}{4b^2} \quad (29)$$

If one substitutes Equation (28) into Equation (29) the following is obtained:

$$\sigma_z = \frac{45M_{(z)}}{14b^2} \quad (30)$$

A summation of moments about point P in Figure 5 is used to find $M_{(z)}^k$.

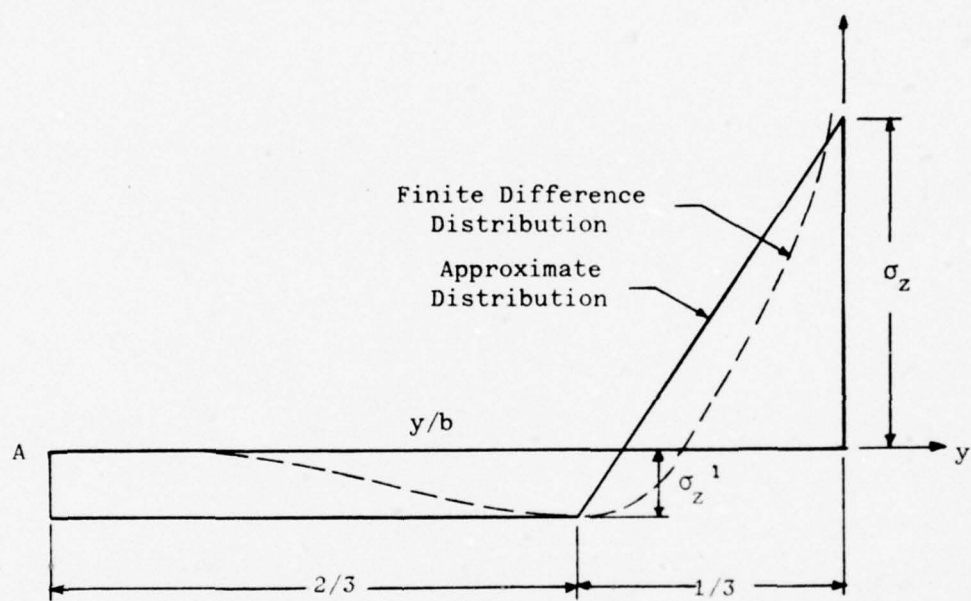


Fig. 6. Distribution of Interlaminar Normal Stress versus y .

$$\begin{aligned}
\Sigma M_p &= 0 \\
-\sigma_y^k(1)(t)(t/2) - \tau_{yx}^k(1)(h)(t) \\
+ M_{(z)}^k - M_{(z)}^{k-1} &= 0 \\
M_{(z)}^k &= M_z^{k-1} + \sigma_y^k(t^2/2) \\
&+ \tau_{yz}^k(t)(h) \quad (31)
\end{aligned}$$

Equations (1) through (31) yield an approximate three dimensional stress field based on laminated plate theory and assumed stress distributions. When thermal stresses are introduced, a particular boundary condition must be applied to maintain the free edges.

The thermal loads, N_x^T , N_y^T , and N_{xy}^T must be applied as tensile stresses inside the specimen. This is done by clamping the free edges for the temperature effect only. Without temperature included σ_z , τ_{yz} , and τ_{xz} at the free edges $z = -h/2$ through $+h/2$ at $y = \pm b$, and $y = -b$ through $+b$ at $z = \pm h/2$ equal zero. These are the imposed boundary conditions incorporated within the computer program to generate the stress field using values σ_x , σ_y , τ_{xy} calculated from experimentally applied loads, N_x or M_x .

Apparent Modulus of Elasticity

Experimental E_{xx} is obtained in the form of a tensile load versus displacement curve. For the tensile test with an applied load, P :

$$\begin{aligned}
E_{xx} \epsilon_x &= \sigma_x \\
&= \frac{P}{bh} \\
\text{or} \quad E_{xx} &= \frac{P}{bh \Delta l} \quad (32)
\end{aligned}$$

where Δl is the measured displacement. The effective modulus of elasticity for tensile loading may be computed analytically from material properties using Hooke's Law. For a tensile load, P

$$N_x = \frac{P}{b} \quad (33)$$

and

$$\epsilon_x = S_{11} N_x \quad (34)$$

where

$$\sigma_x = \frac{N_x + N_x^T}{h} \quad (35)$$

$$\epsilon_x = [A]^{-1} N_x \quad (36)$$

$$S_{11} = \frac{1}{\bar{E}_{xx}} \quad (37)$$

or

$$E_{xx} = \frac{N_x + N_x^T}{h[A_{11}]^{-1} N_x} \quad (38)$$

This is the apparent tensile modulus of elasticity computed from material properties. Similarly, using the $[D]$ matrix, an apparent bending modulus of elasticity may be computed.

The deflection measured experimentally in a four point loading apparatus is the displacement at the point, $L/4$, where the load is applied. This is the crosshead displacement on the Instron machine. Since the bending specimens have a high length-to-width ratio, it can be assumed that

$$w = w(x) \quad (39)$$

therefore

$$\frac{d^2 w}{dx^2} = -\frac{M}{EI} \quad (40)$$

Integrating Equation (40) where P is the load applied by the Instron crosshead and w is the deflection at the quarter point yields

$$\bar{E} = \frac{Pl^3}{8wbh^3} \quad (41)$$

If shear deformation is included, Whitney [23] shows that

$$\bar{E} = \frac{Pl^3}{(8bh^3w - \frac{Plh^2}{kG})} \quad (42)$$

(See Appendix A for development). A value of $k = 5/6$ is used as suggested by Whitney and Pagano [26] and \bar{G} is a function of the material property term, G_{31} . From material properties and an applied bending moment, M_x , an analytical value of \bar{E}_{xx} may be determined using Equation (40), the laminated plate theory previously developed, and the following,

$$\begin{aligned} k_x &= [D_{11}]^{-1} M_x \\ &= - \frac{\partial^2 w}{\partial x^2} \end{aligned} \quad (43)$$

and

$$M = bM_x \quad (44)$$

then

$$\bar{E}_{xx} = \frac{12}{h^3 [D_{11}]^{-1}} \quad (45)$$

Another comparative value of \bar{E}_{xx} may be computed using laminated beam theory and material properties of the various layers.

For symmetrically layered beams, the bending stiffness, EI , can be replaced by an equivalent stiffness, $\bar{E}_{xx}I$, defined in the following

manner [23]:

$$\bar{E}_{xx} I = \sum_{k=1}^N E_{xx}^k I^k \quad (46)$$

where E_{xx}^k and I^k are characteristics of any k th layer relative to the beam axis and I is the moment of inertia of the beam relative to the midplane.

This study will compare values calculated from experimental data using Equations (32) and (41) with values computed with Equations (38), (42), (45), and (46).

III. Results

This section contains the compilation of results from the different applications of this thesis study. A computer program was created which utilized classical laminate theory and computation methods of Section II to calculate a three dimensional stress field approximation. The parts concern verification of the program and the stress distribution assumptions of Pipes and Pagano [13], application of thermal residual stresses, and effects of introducing hybrid lamina into non-hybrid laminates, results of work with the 48 ply hybrid laminates, and Tsai-Hill failure criteria applicability.

Verification of Computer Program

A. Pipes and Pagano Assumption.

The laminate geometry by Pipes and Pagano [13] was input into the program to see if a similar maximum value of the interlaminar normal stress, σ_z , could be obtained. Pipes and Pagano state that a maximum value of 10,000 psi was predicted by their finite difference study. The program predicted a value of 10,961 psi which is within 10 percent of Pipes and Pagano's value and thus within possible roundoff associated with the stress of 10,000 psi.

B. Thermal Stress Distribution.

The second portion of the computer program concerned the assumed thermal residual stress distribution throughout a specimen. The thesis study assumes that thermal residual stresses, σ_x , σ_y , and τ_{xy} , are distributed evenly across the face on which they act. The residual thermal interlaminar shear stresses, τ_{xz} and τ_{yz} , have been conveniently approximated in the free edge effect manner. The interlaminar normal thermal residual stress, σ_z , is distributed as in

Figure 6 which the author feels is a valid approximation for a first attempt. This study further assumes that this stress distribution is valid for all ply orientations. Recent finite element studies [20] propose that the stress distribution varies with different ply orientations. Specimen geometries used by Wang and Crossman [20] were incorporated as input into the program with no applied loads and a ΔT equal to 1°F . For $(0^{\circ}, 90^{\circ})$ s and $(90^{\circ}, 0^{\circ})$ s specimens (see Appendix B), values for the maximum stresses σ_x , σ_y , τ_{xz} , τ_{xy} , and σ_z , achieved by the thesis program, are comparable to those achieved by Wang and Crossman even though the distribution of the stress field was not as refined as the one projected in Ref [20]. The value of τ_{yz} predicted by the thesis program was within 35 percent of the value predicted by the finite element method. Values of τ_{xy} and τ_{xz} for the $(\pm 45^{\circ})$ s specimen did not agree with those of [20]. These discrepancies may be partially explained in that the finite element study showed that the free edge effect depth was four times greater for thermal stresses than the previous assumed depth [13, 20]. The distribution used in this study seems adequate for the cross ply orientations of 0° and 90° . The distribution obtained by the finite element method in the $(\pm 45^{\circ})$ s case contained points of discontinuity. The area of thermal stress distribution apparently is open for further research. With these considerations, the approximation technique utilized in this study and the values obtained for the $(\pm 45^{\circ})$ s geometry are valid approximations.

Thermal residual stresses become important factors to consider as is demonstrated by the next portion of this section.

Effects of Addition of Hybrid Material

This portion of study was designed to give some preliminary insight into the behavior of composite laminates as hybrid material lamina are introduced into the laminate. Significant changes in stress field and effects of changes in the overall material properties of the laminate were points of primary interest. Two specimen geometries were selected, one for general study and another for specific study of material property changes.

A. Eight Ply Specimen

The most commonly used laminate configuration was the basis for the specimen geometry to be used in this portion. A symmetric eight ply laminate, composed of graphite epoxy with characteristics described in Appendix B, was selected with ply orientations of $(0^\circ, \pm 45^\circ, 90^\circ)_s$. Five cases were run under the same tensile and flexure loading and temperature conditions. A hybrid lamina of 80 percent graphite epoxy and 20 percent glass epoxy material was introduced in Cases II through V respectively as follows:

- | | |
|----------|---|
| Case I | All graphite epoxy |
| Case II | 0° ply of Case I replaced with hybrid material |
| Case III | $+45^\circ$ ply of hybrid material |
| Case IV | -45° ply of hybrid material |
| Case V | 90° ply of hybrid material |

To evaluate the significance of the thermal residual stress effect, a $\Delta T = 0^\circ\text{F}$ was applied and compared with a $\Delta T = -200^\circ\text{F}$, a condition that might be anticipated in an environmentally uncontrolled testing laboratory. The maximum value of the interlaminar normal stress, σ_z , is compared for each case in the following table.

Table I
Maximum Value of Interlaminar Normal Stress, σ_z ,
With Applied Load, $N_x = 2100$ lb/in.

Case	$\Delta T = 0^\circ\text{F}$ σ_z (psi)	$\Delta T = -200^\circ\text{F}$ σ_z (psi)
I	-1041	3478
II	-1194	2951
III	-1009	3501
IV	-1018	3526
V	- 961	3202

The maximum value of σ_z occurred at the top of lamina four in each case. Inclusion of the thermal residual stress can be a significant factor in specimen analysis as illustrated in Table I. The sign reversal shows that σ_z is now a delaminating stress. The values in Table I, with temperature considered, are approximately 18 percent of the applied load. This situation is a potential failure mechanism since the ultimate strength of most composite materials in the z direction is approximately 5 percent of the ultimate strength in the longitudinal material property direction. With temperature effects included, the specimen essentially is no longer loaded uniaxially but biaxially. Thermal stresses were included in all subsequent computations for this study.

The effects of replacing the lamina in Case I with a hybrid lamina in Cases II through V on the stress fields are illustrated in Figures 7 through 12 for the tensile loading. (The curves illustrated in Figures 9, 11, 12, 15, and 16 are shown with parabolic

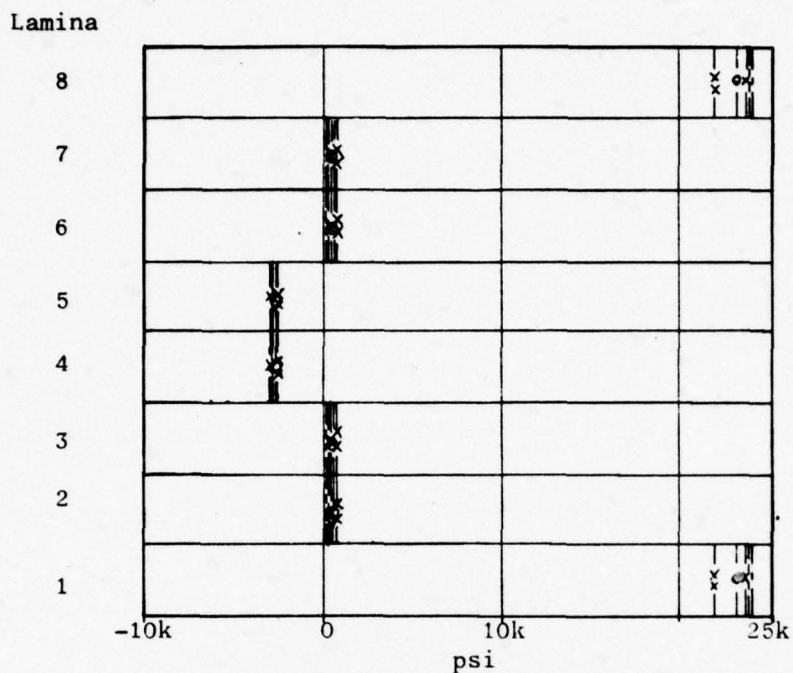


Fig. 7. Distribution of σ_x in 8 ply Laminate -
Tensile Load, N_x

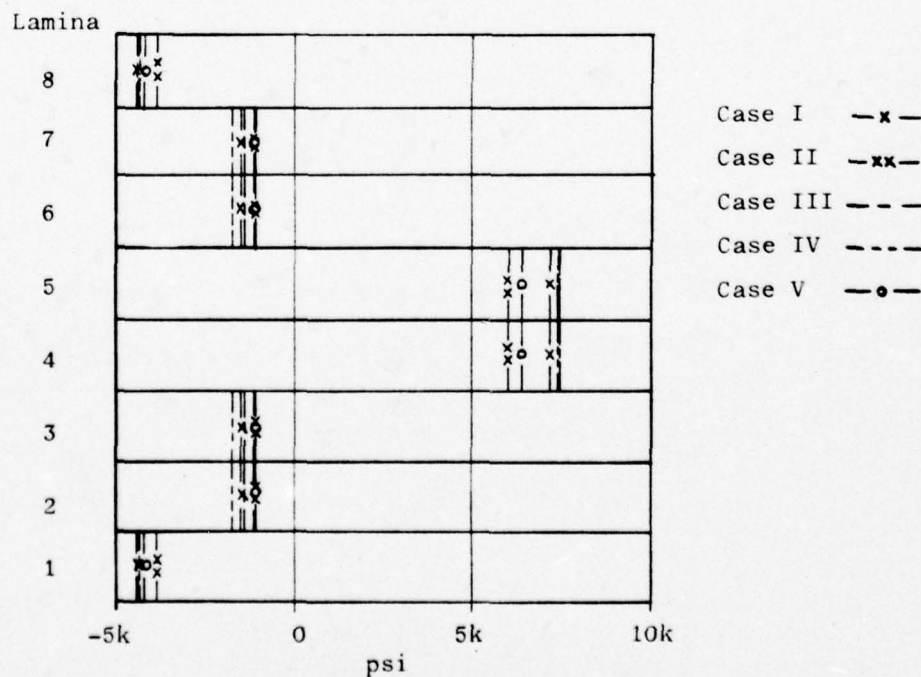


Fig. 8. Distribution of σ_y in 8 ply Laminate -
Tensile Load, N_x

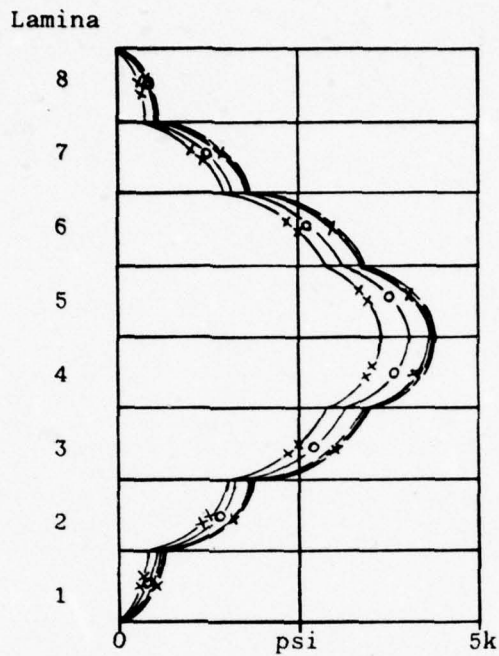


Fig. 9. Distribution of σ_z in 8 ply Laminate - Tensile Load, N_x

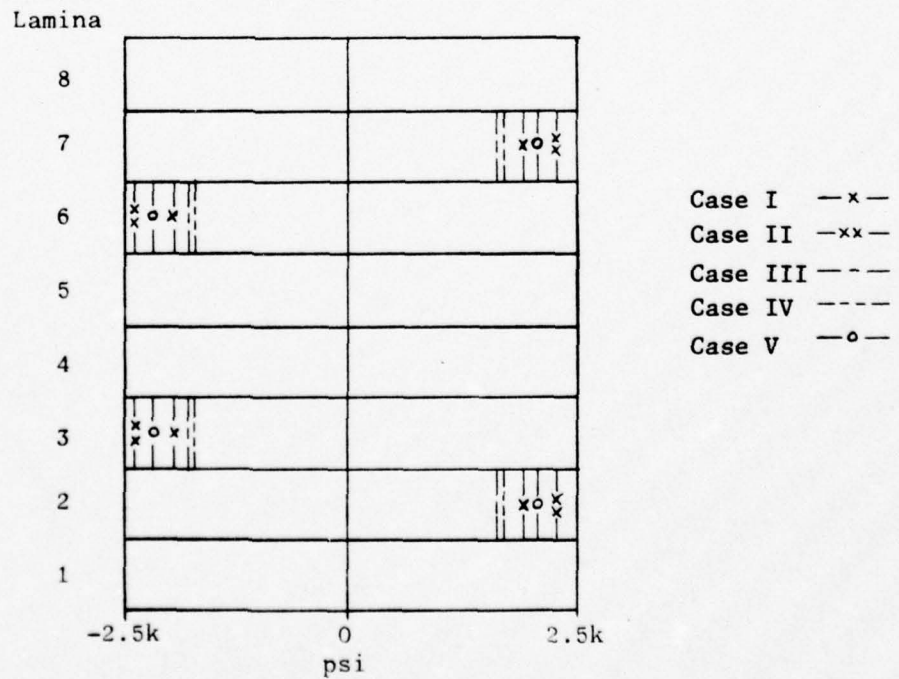


Fig. 10. Distribution of τ_{xy} in 8 ply Laminate - Tensile Load, N_x

Lamina

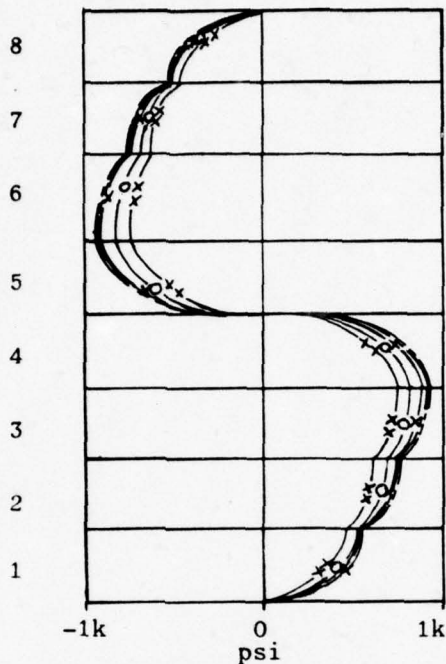
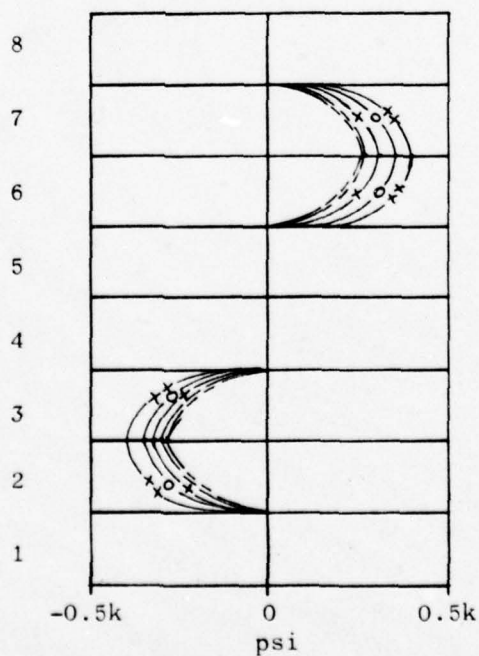


Fig. 11. Distribution of τ_{yz} in 8 ply
Laminate - Tensile Load, N_x

Lamina



- Case I —x—
- Case II —xx—
- Case III ----
- Case IV - - - -
- Case V —o—

Note:

Stresses not shown
are negligible and
taken to equal to
zero.

Fig. 12. Distribution of τ_{xz} in 8 ply
Laminate - Tensile Load, N_x

through-the-lamina distribution even though calculated values have been determined for the upper and lower surfaces of each lamina only). In most cases σ_x , σ_y , σ_z , and τ_{yz} were reduced by 8 to 10 percent when the hybrid lamina was placed in the 0° and 90° orientations. On the other hand, τ_{xy} and τ_{xz} increased by approximately 20 percent. When the hybrid lamina was placed in the $\pm 45^\circ$ plies, σ_x , σ_y , σ_z , and τ_{yz} remained essentially unchanged while the shear stresses τ_{xy} and τ_{xz} were reduced approximately 13 percent. The tensile modulus of elasticity, \bar{E}_x , predicted by laminated plate theory was reduced by 8 percent in Case II and only 1.5 percent for Cases III through V as shown in the following table.

Table II
Effective Tensile Modulus of Elasticity, \bar{E}_x

Case	\bar{E}_x (psi)
I (all graphite epoxy material)	7.34×10^6
II (0° ply of hybrid material)	6.67×10^6
III ($+45^\circ$ ply of hybrid material)	7.23×10^6
IV (-45° ply of hybrid material)	7.23×10^6
V (90° ply of hybrid material)	7.23×10^6

The flexure loading study yields stresses, due to ΔT , that are not symmetric with respect to the midplane of the specimen. See Figures 13 through 16. (τ_{xz} and τ_{xy} distributions are not plotted due to their small values.)

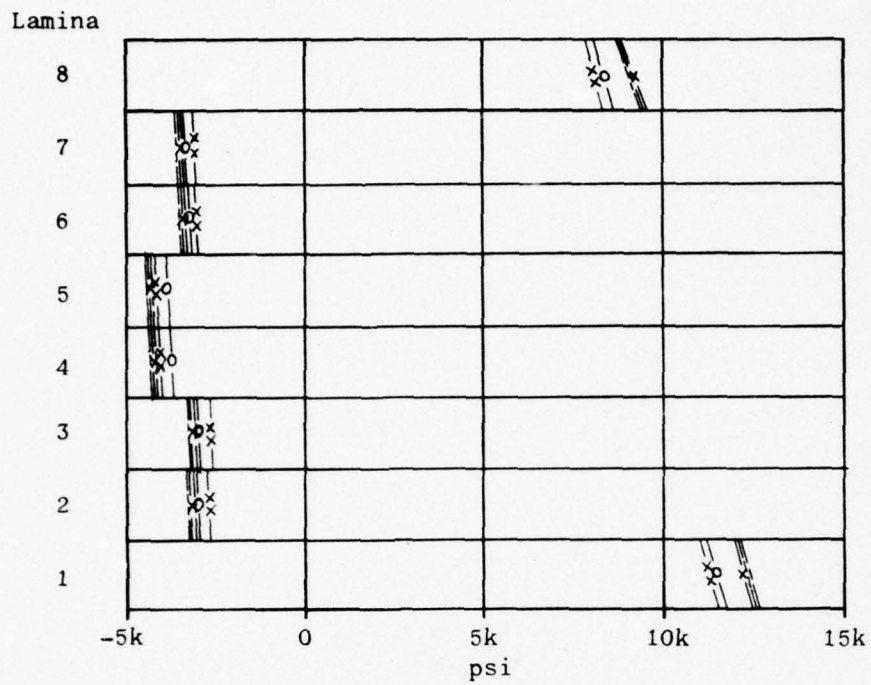


Fig. 13. Distribution of σ_x in 8 ply Laminate - Flexure Load

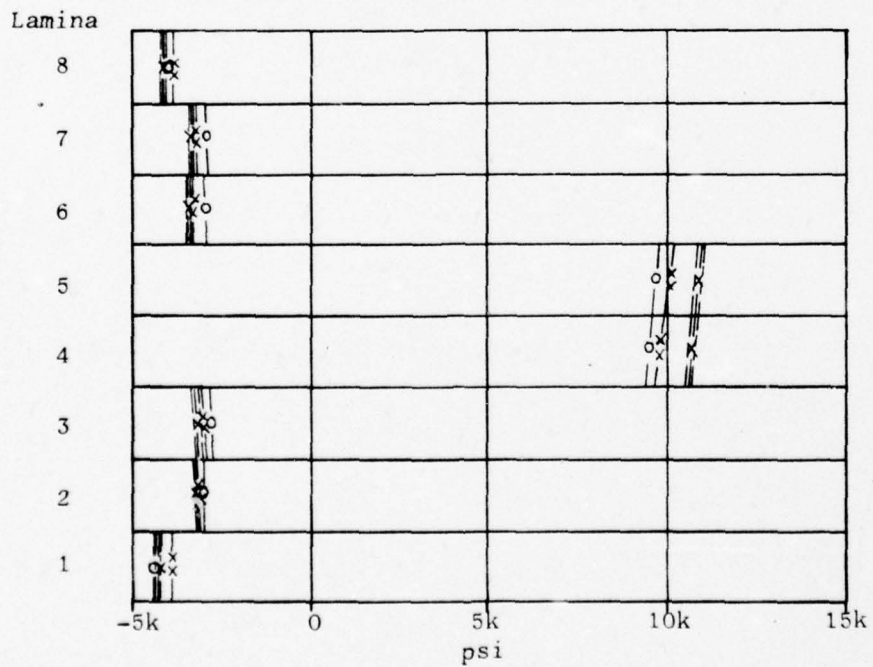


Fig. 14. Distribution of σ_y in 8 ply Laminate - Flexure Load

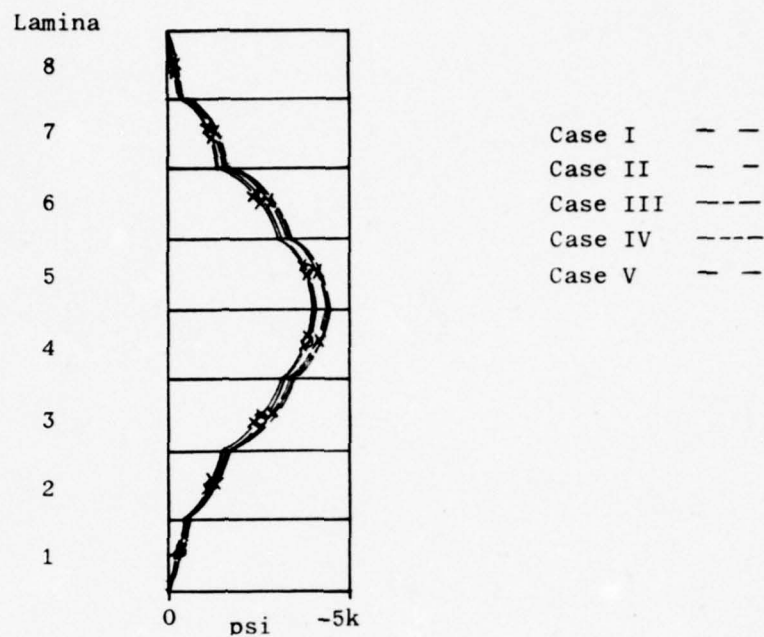


Fig. 15. Distribution of σ_z in 8 ply Laminate - Flexure Load

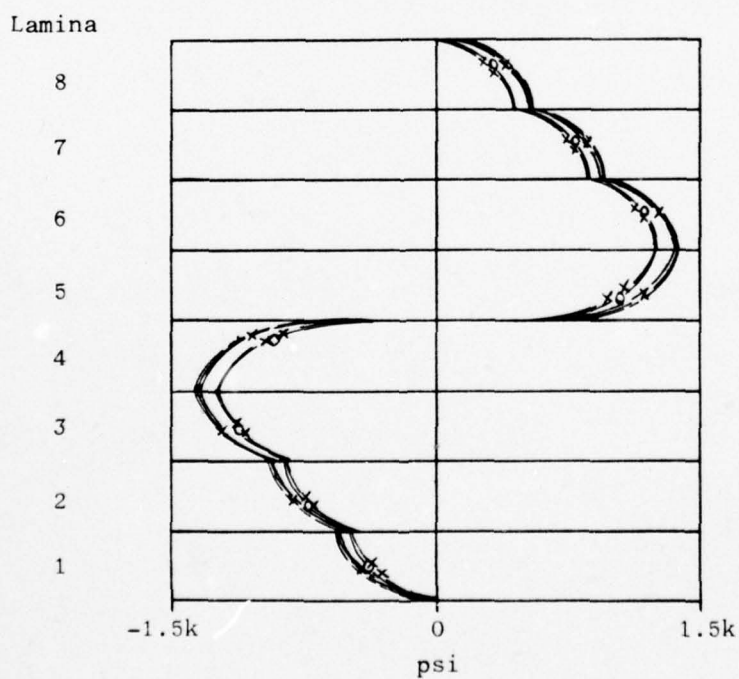


Fig. 16. Distribution of τ_{yz} in 8 ply Laminate - Flexure Load

For small applied loads the upper fibers are generally in compression according to beam theory. The case is reversed with temperature effects in the analysis. The upper fibers may not encounter compressive forces until much larger applied flexure loads. When considering maximum values of stress encountered in the flexured specimen, the shear stresses, τ_{xz} and τ_{xy} , were relatively insignificant. σ_x , σ_y , σ_z , and τ_{yz} were reduced by 5 to 15 percent in Cases II and V and were relatively unchanged in Cases I, III, and IV. The τ_{xy} and τ_{xz} stresses, even though small, increased in Cases III and IV. This result is reversed from that of the tensile loaded case. The maximum interlaminar normal stress, σ_z , encountered, was approximately 30 percent of the maximum stress, σ_x , occurring in the outer fibers.

The effective bending modulus of elasticity, \bar{E}_x , responded in the same manner as the tensile modulus of elasticity. \bar{E}_x was reduced by 12 percent for Cases II but remained unchanged for all other cases. The change in the modulus, \bar{E}_x , in Case II for both tensile and flexure loading was due to placing the hybrid in the 0° ply orientation where its smaller material property values have the greatest overall effect.

B. Twelve Ply Specimen

The second analytical specimen geometry was selected for its similarity to the orientations of the actual 48 ply specimens. This specimen was a twelve ply symmetric laminate with orientations of $(\pm 45^\circ, 0^\circ, 0^\circ, \pm 35^\circ)_s$. This smaller number of plies is generally used in experimental determination of material properties. Two cases of this specimen were investigated (see Appendix B). Case I had the $\pm 35^\circ$ plies composed of hybrid material with all other plies of glass epoxy.

Case II had the $\pm 45^\circ$ plies of glass epoxy with all other plies of hybrid material. The effect of hybridization on the flexure modulus of elasticity was investigated considering several different methods of calculation. Values for the modulus were computed using laminated beam theory as expressed in Section II. (This approach is a general design technique because of its simplicity.) There are two possible procedures when using this method. The first is to calculate the modulus by using material property values that have not been transformed into the load axes system. The second uses transformed material property values in calculations. A third value for the flexure modulus was calculated using composite laminate theory. Table III illustrates the values obtained by the three methods.

Table III
Effective Flexure Modulus of Elasticity (psi)

Case	Non-Oriented Beam Theory	Oriented Beam Theory	Composite Laminate Theory
I	1.31×10^8	6.54×10^7	3.26×10^6
II	1.76×10^8	1.18×10^8	5.69×10^6

As can be surmised, large errors are inherent in using laminated beam theory particularly when not using the proper axis system rotation. The values for Cases I and II obtained by composite laminate theory are closer to those anticipated from experimental results. Replacing the 0° oriented plies in Case I by hybrid material had a significant effect on the effective modulus as evidenced by the 74 percent increase in value.

The significance of the shear contribution to the deflection was the other aspect considered with these specimen geometries. Using theory developed in Appendix A, the expected deflection, w , of a specimen under four point flexure loading was calculated with and without the shear contribution term included. The results are listed in Table IV.

Table IV
Analytical Deflection of Beam Specimen With and Without
Shear Load at Quarter Points = 100 lbs.

Case	w , in. (Eq. 41) (Shear not included)	w' , in. (Eq. 42) (Shear included)	Percent Difference
I	0.02960	0.02966	1.9
II	0.01600	0.01656	3.5

In both cases the percentage of total deflection due to shear distortion can be neglected as might be expected since theoretically shear exists up to the quarter load points but not between them. The apparent increased contribution in Case II is caused by the decrease in value of the $[D_{11}]^{-1}$ term while the $[A_{55}]$ term remained unchanged for this particular geometry.

The results of testing an actual hybrid composite laminate are the only means to verify the above analytical results. For this study, the available test specimens were 48 ply rather than twelve ply specimens. The 48 ply specimen was manufactured for proposed use in turbo fan blades where the expected minimum thickness encountered at the blade tip would be 48 plies. The test results should indicate if thicker

hybrid laminates can be properly characterized by test specimens of more normal thickness.

Experimental Results With 48 ply Specimens

Both tensile and four point flexure test were performed on two 48 ply specimens configured as described in Appendix B. The intent of the experimental testing was primarily to determine how closely hybrid composite laminates obey classical laminate theory and secondly to determine if hybrids are subject to the same limitations of characterization as other composite laminates. These limitations are manifested in the different values obtained for a modulus of elasticity by tensile and flexure tests. The effect of shear distortion on deflection measurements and determination of stress fields by use of the thesis computer program were sideline studies.

The availability of test specimens was limited by supply of material, therefore the width to depth ratio of the test specimen was only two to one. Ideally, to minimize free edge effect stress influence, the minimum ratio should be four to one. Therefore, the interlaminar surfaces of these specimens were entirely in the regime of free edge effect.

Load-displacement curves were plotted during testing by use of Instron testing machinery. (See Figures 17 and 18). The results of the thesis computer program showed that interlaminar shear stresses and normal stresses were insignificant when compared to the other stresses in each lamina. Even at stress levels experienced at specimen separation, neither the interlaminar shear nor normal stresses were high enough within themselves to be a failure factor.

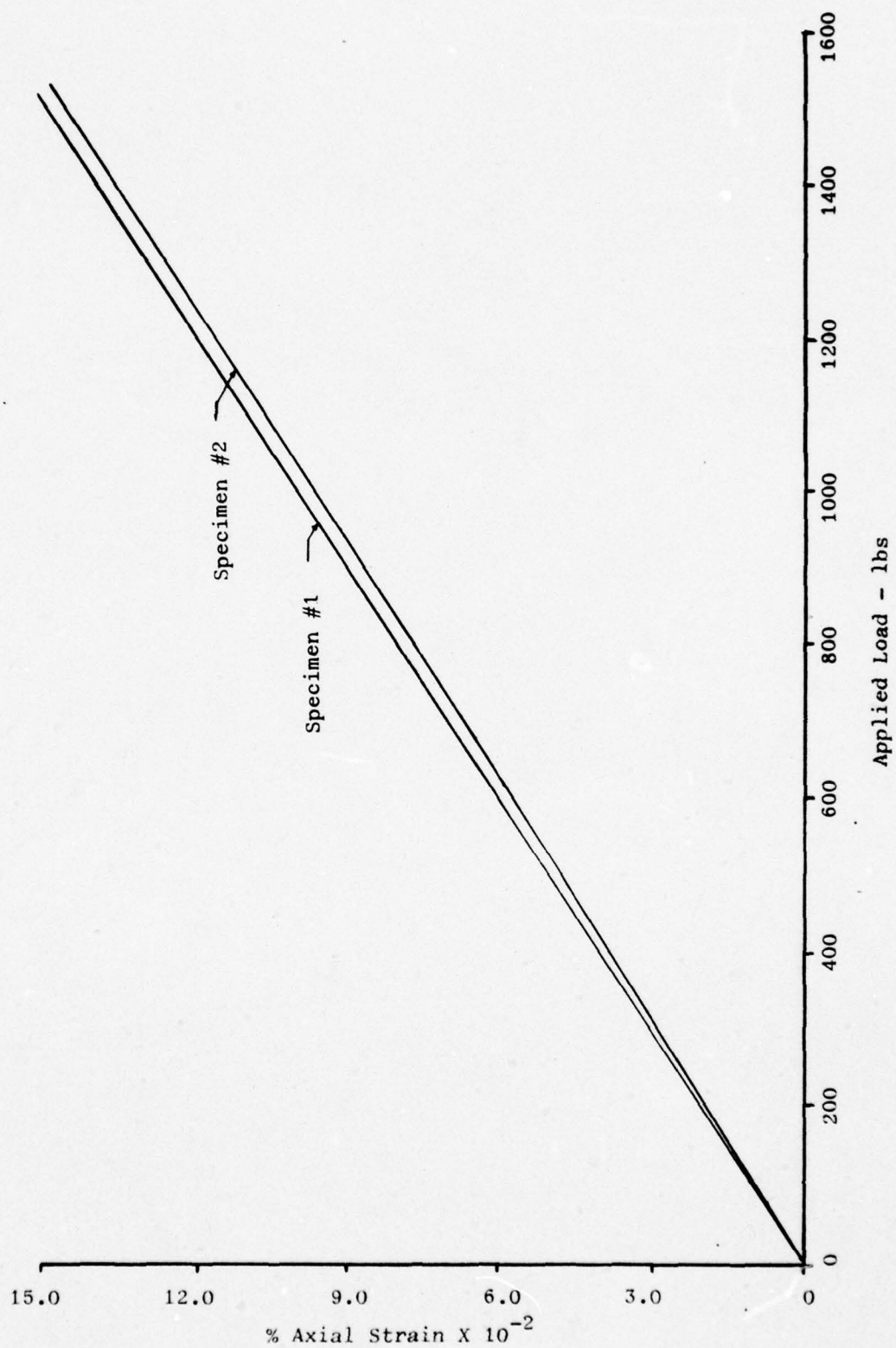


Fig. 17. Experimental Load-Displacement Curves for 48 ply Specimens Under Tensile Load

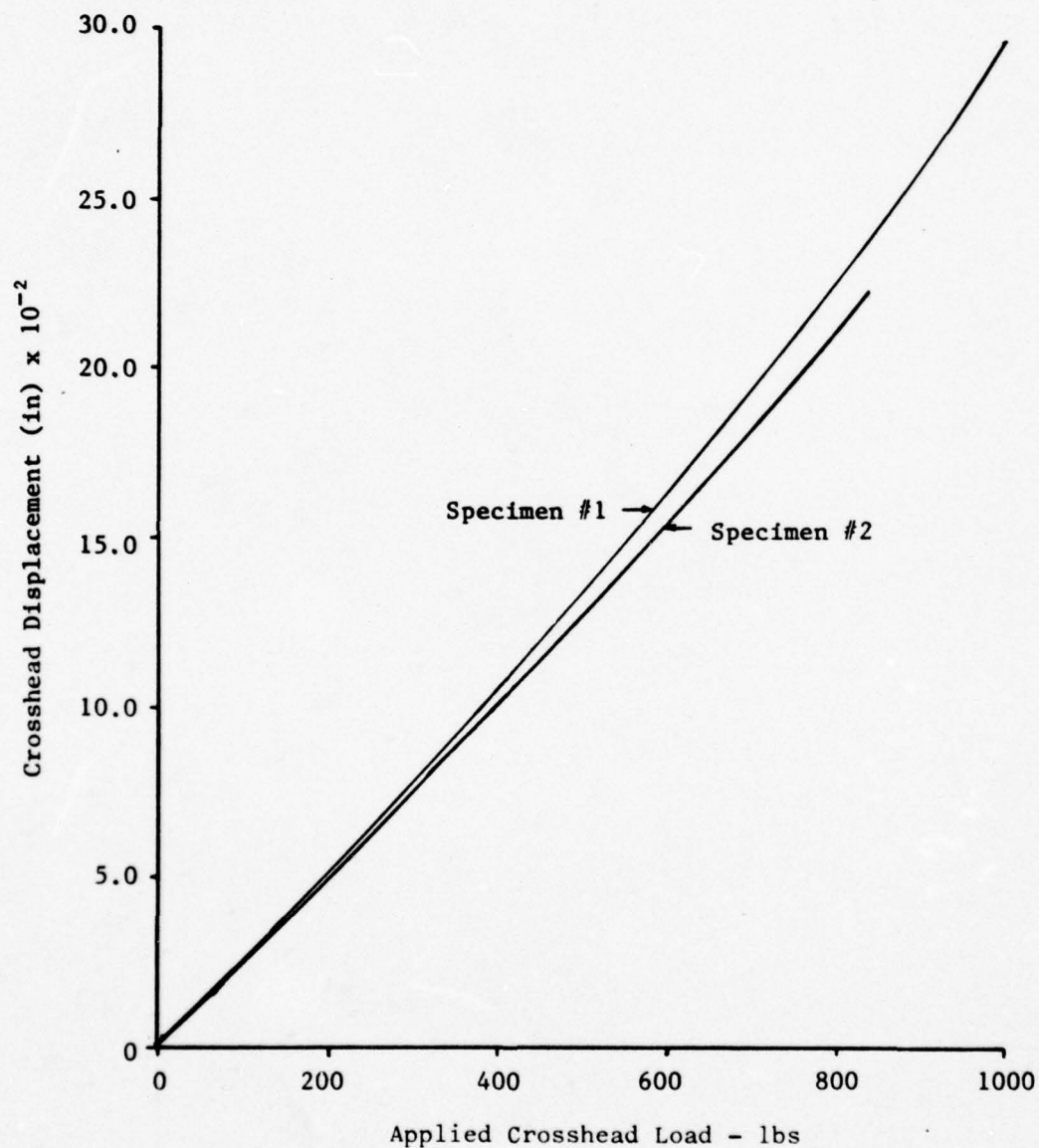


Fig. 18. Experimental Load-Deflection Curves for 48 ply Specimens Under Flexure Load

The results of analytical and experimental determination of material properties are presented in Table V.

Table V
Modulus of Elasticity $\times 10^6$

	Specimen #1	Specimen #2
Experimental Tensile	8.9	7.5
Analytical Tensile	9.1	7.5
Analytical Tensile and Temperature	9.8	8.1
Experimental Bending	4.3	4.7
Analytical Bending	4.7	6.4
Beam Theory (Oriented)	3.6	5.5
Beam Theory (Non-Oriented)	9.4	11.1

The 48 ply specimens have so many layers that they approach homogeneity. This is apparent by a comparison of the values for the modulus predicted by the analytical bending method and the beam theory oriented case. As expected, specimen #2 was stiffer than #1 because eight 0° plies of glass epoxy were replaced with plies of hybrid material. The fallacy of using modulus values predicted by laminated beam theory is apparent, particularly when the lamina material properties are not correctly oriented prior to computation. The only anomaly in comparing analytical and experimental data was the experimental value obtained for the flexure modulus of elasticity for specimen #2. The value is approximately 27 percent less than that predicted by laminated plate theory. A possible explanation for this may be in the consistency of the

specimen. Since the 80-20 material is made in ribbon fashion and then laminated with other 80-20 ribbon plies, the possibility of narrow specimens being cut from an area where glass fibers are highly concentrated exist. The second specimen, in effect, would be similar to the first, and therefore the former would exhibit characteristics similar to the latter.

It is evident that caution must be exercised in specimen preparation when utilizing hybrid materials. The widely different values of bending and tensile moduli make it apparent that, in depicting stress fields within hybrid composite laminates, the appropriate material \bar{E}_{xx} should correspond to the general load situation.

The shear coupling effect, as discussed with the twelve ply model, was less than two percent for these specimens and therefore insignificant. However, as predicted by the twelve ply model, the percentage of the shear contribution to deflection increased with specimen #2. It appears that characteristic results experienced in thinner test specimens of hybrid material, i.e., the twelve ply specimen, are indicative of characteristics experienced in thicker hybrid laminates. The impact on characteristic behavior by changes in configuration is somewhat lessened in thicker specimens by the influence of increasing homogeneity.

Application of Tsai-Hill Failure Criteria to Hybrid Composites

The thesis program increased the applied tensile and flexure loads in increments of 100 lb/in. and 12.5 lb-in. respectively. After each increment the Tsai-Hill criteria was applied to each lamina of the 48 ply specimens (see Appendix B). Upon failure of this criteria by any lamina the program was stopped. This procedure yielded an applied load

at which first lamina failure was encountered. It must be pointed out that the term, failure, in this connotation does not infer complete lamina separation, but either the matrix or fiber material or a combination of both has exceeded an ultimate strength. This may be interpreted as initial onset of failure.

Table VI indicates the particular failed lamina and the applied loads at failure for the 48 ply specimens #1 and #2.

Table VI
Predicted Loads at First Lamina Failure

48 ply Specimen	Tensile Load (lbs.)	Flexure Load (lbs.)	Approximate Experimental Load	Failed Lamina
#1	1359		>2000	1
		100	210	5
#2	1333		1200	1
		125	230	8

For the tensile load applications, experimental verification was somewhat difficult. Load-displacement curves for specimen #1 were linear up to a tensile load of 2000 lbs (see Figure 17) with ultimate failure (specimen separation) at about 10,000 lbs (not shown on Figure 17). There was no evidence of first ply failure at the predicted load of 1359 lbs. The tensile load-displacement curve for specimen #2, however, showed a definite trend toward non-linearity in the 1200-1400 lb range. This was taken as confirmation of the failure load, 1333 lbs, as predicted by the Tsai-Hill criteria.

The flexural load displacement curves for specimens #1 and #2 (see Figure 18) began to be non-linear after applied loads of 210 lbs and 230 lbs, respectively. This difference in itself is not particularly significant due to the fact that the failure criteria incorporated into the calculation is a two-dimensional criteria (the actual stress failure mechanism maybe three dimensional in nature) and stress calculations are based on two-dimensional laminated plate theory with the corresponding limitations.

Consequently, the true stress field in a flexure test, including temperature effects, as applied to failure of the specimen, should probably be calculated with a more rigorous technique which may not be available at present. Because of these facts, this author concludes that the results pertaining to the specimen failure analysis are reasonable, though conservative, approximations and demonstrate the usefulness of the Tsai-Hill criteria in conjunction with laminated plate theory.

IV. Conclusions

The following conclusions, considering hybrid composite laminates of the type described in this thesis, can be made.

- (1) Classical laminate theory yields reasonable values for the tensile and flexure moduli of elasticity for these hybrid laminates. Values obtained by laminated beam theory, particularly when using non-oriented material properties, are not adequate for characterizing the flexure modulus of elasticity.
- (2) Values for the tensile and flexure moduli should be used only in the respective loading situations for accurate stress analysis.
- (3) Hybridization, as studied in this thesis, has little effect in changing material property characteristics. The benefits, the basis for the original hybridization, outweigh any degradation encountered. Most, if any, degradation occurs when the hybrid is placed in the 0° and/or 90° orientations.
- (4) Interlaminar shear stresses and normal stresses should be investigated in the initial design of a hybrid laminate, particularly if the laminate contains 90° ply orientations. Load shear distortion is insignificant in the type of hybrid laminates investigated.
- (5) Thermal residual stresses are significant and should be considered in data reduction for accurate stress analysis.
- (6) The Tsai-Hill failure criteria seems to be applicable to hybrid composites and provides rough approximations of first ply failure in tensile and flexure test. It is, however, limited due to its inaccuracy in what appears to be a three dimensional

problem.

- (7) Caution must be exercised in preparation of test specimens to insure that dimensions are adequate in order to reduce the free edge effects and to insure an adequate dispersion of any peculiar material configuration characteristics.

Bibliography

1. Ashton, J. E., J. Halpin, and P. Petit. Primer on Composite Materials: Analysis. Westport, Conn.: Technomic Publishing Company, Inc., 1969.
2. Ashton, J. E., and J. M. Whitney. Theory of Laminated Plates. Stanford, Conn.: Technomic Publishing Company, Inc., 1970.
3. Halpin, J. C. and R. L. Thomas. "Ribbon Reinforcement of Composites." Journal of Composite Materials, 2: 488-497 (October, 1968).
4. Hill, R. The Mathematical Theory of Plasticity. London: Oxford University Press, 1950.
5. Hsu, P. W. and C. T. Herakovich. Interlaminar Stresses in Composite Laminates -- A Perturbation Analysis. NASA-CR-148080. VPI-E-76-1. January, 1976.
6. Jones, R. M. Mechanics of Composite Materials. New York: McGraw-Hill Book Company, 1975.
7. Lipshitz, J. M. "Impact Strength of Angle Ply Fiber Reinforced Materials." Journal of Composite Materials, 10: 92-101 (January, 1976).
8. Mair, A. Analysis of Beam Bending Experiments on Off-Axis Laminated Composites. Unpublished thesis. Wright-Patterson Air Force Base, Ohio: Air Force Institute of Technology, March 1972.
9. Pagano, N. J. "Analysis of the Flexure Test of Bidirectional Composites." Journal of Composite Materials, 1: 336-342 (1967).
10. Pagano, N. J. and R. Pipes. "Some Observations on the Interlaminar Strength of Composite Laminates." International Journal of Mechanical Science, 15: 679-688 (1973).
11. Pagano, N. J. and S. W. Tsai. "Micromechanics of Composite Materials." Composite Materials Workshop. Stanford, Conn.: Technomic Publishing Company, Inc., 1968.
12. Pipes, R. B. and Pagano, N. J. "The Influence of Stacking Sequence on Laminate Strength." Journal of Composite Materials, 5: 50-56 (January, 1971).
13. Pipes, R. B. and N. J. Pagano. "Interlaminar Stress in Composite Laminates Under Uniform Axial Extension." Journal of Composite Materials, 4: 538-548 (October, 1970).

14. Puppo, A. H. and Eversen, H. A. "Interlaminar Shear in Laminated Composites under Generalized Plane Stress." Journal of Composite Materials, 4: 204-220 (April, 1970).
15. Spies, G. J. and deJong, T. "Determination of Elastic Constants of a Unidirectionally Reinforced Plastic." AGARD-CP-63-71, NATO. AGARD Conference Proceedings No. 63 on Composite Materials.
16. Tang, S. "Interlaminar Stresses in Uniformly Loaded Rectangular Composite Plates." Journal of Composite Materials, 10: 69-77 (January, 1976).
17. Tsai, S. W. and Pagano, N. J. "Invariant Properties of Composite Materials." Composite Materials Workshop. Stanford Conn.: Technomic Publishing Company, Inc., 1968.
18. Tsai, S. W. "Fundamental Aspects of Fiber Reinforced Plastic Composites." in Strength Theories of Filamentary Structures, edited by R. T. Schwartz and H. S. Schwartz. New York: Wiley Interscience, 1961.
19. Waddoups, M. E. "Characterization and Design of Composite Materials." Composite Materials Workshop. Stanford, Conn.: Technomic Publishing Company, Inc., 1968.
20. Wang, A. S. D. and Crossman, F. W. "Edge Effects on Thermally Induce Stresses in Composite Laminates." Journal of Composite Materials, 11: 300-312 (July, 1977).
21. Wang, A. S. D. and Crossman, F. W. "Some New Results on Edge Effects in Symmetric Composite Laminates." Journal of Composite Materials, 11: 92-106 (January, 1977).
22. Whitney, J. M. "Analytical and Experimental Methods in Composite Mechanics." Journal of Composite Materials: 398-411 (July, 1969).
23. Whitney, J. M., Browning, C., and Mair, A. "Analysis of the Flexure Test for Laminated Composite Materials." Composite Materials Testing and Design (Third Conference), ASTM STP 546: 30-45 (1974).
24. Whitney, J. M. and Dauksys, R. J. "Flexure Experiments on Off-Axis Composites." Journal of Composite Materials, 4: 135-137 (January 1970).
25. Whitney, J. M. and Browning, C. "Free Edge Delamination of Tensile Coupons." Journal of Composite Materials, 6: 300-303 (April, 1972).

26. Whitney, J. M. and Pagano, N. J. "Shear Deformation in Heterogeneous Anisotropic Plates." Journal of Applied Mechanics, 37: 1031-1036 (December 1970).

Appendix A

Transverse Shear Deformation

Since the shear direction of a composite material generally has the lowest ultimate strength, then transverse shear deformation can be considerable in flexure loaded specimens and should be accounted for in data reduction.

Using Figure 18, the displacement of any point above the neutral axes of a beam under flexural loading can be written as:

$$u = u^0(x,y) + z \psi_x(x,y) \quad (A1)$$

where $w = w(x,y) \quad (A2)$

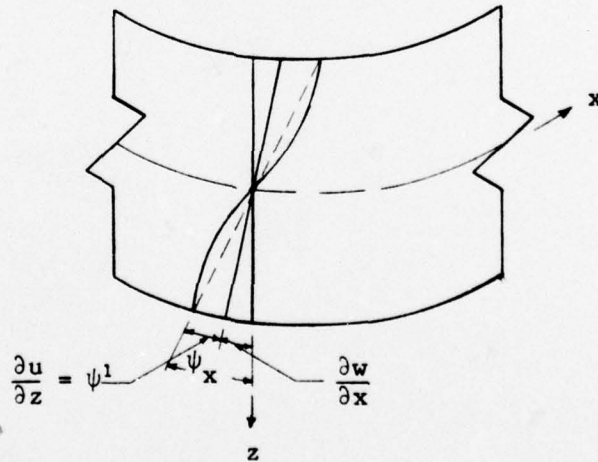


Fig. 19. Section of a Flexure Loaded Beam

The shear strain, γ_{xz} , is given by:

$$\begin{aligned}\gamma_{xz} &= \frac{\partial u}{\partial z} + \frac{\partial w}{\partial x} \\ &= \psi_x^1 + \frac{\partial w}{\partial x}\end{aligned}\quad (A3)$$

For the classical case where $\gamma_{xz} = 0$, then

$$\frac{\partial w}{\partial x} = -\psi_x^1 \quad (A4)$$

Therefore ψ_x is the total rotation including $\frac{\partial w}{\partial x}$ and shear deformation or ψ_x is the change of slope of the normal to the undeformed plane.

From the laminate constitutive relationships [5,25], the shear per unit width on the x-face is

$$Q_x = kA_{55} \gamma_{xz} \quad (A5)$$

where $k = 5/6$. Equation (A5) in conjunction with Equation (A4) gives

$$Q_x = kA_{55} \left(\frac{\partial w}{\partial x} + \psi_x^1 \right) \quad (A6)$$

where A_{55} is defined in Section II. From Section II the following relationship is expressed

$$\begin{Bmatrix} k_x \\ k_y \\ k_{xy} \end{Bmatrix} = [D]^{-1} \begin{Bmatrix} M_x \end{Bmatrix} \quad (A7)$$

where

$$\begin{aligned}k_x &= -\frac{\partial^2 w}{\partial z^2} \\ &= \frac{\partial \psi_x^1}{\partial x}\end{aligned}\quad (A8)$$

Equilibrium considerations from laminated plate theory yield

$$\frac{\partial M_x}{\partial x} + \frac{\partial M_{xy}}{\partial y} - Q_x = 0 \quad (A9)$$

but for this case $M_{xy} = 0$ therefore Equation (A9) becomes

$$\frac{\partial M_x}{\partial x} - Q_x = 0 \quad (A10)$$

The following relationship is also given in Section II:

$$\frac{d^2 w}{dx^2} = - \frac{M}{EI} \quad (A11)$$

where $\bar{E} \equiv \frac{12}{h D_{11}^{-1}}$, $M = b M_x$. If one substitutes Equation (A8) into Equation (A11), the result is

$$\frac{\partial \psi^1}{\partial x} = \frac{M}{EI} \quad (A12)$$

The function ψ^1 can be found by integrating Equation (A12). These expressions in conjunction with Equation (A10) give an equation that may be integrated to yield an expression for the deflection, w , as follows:

$$w = \frac{Px}{2bkA_{55}} - \frac{D_{11}^{-1}P}{b} \frac{x^3}{12} - \frac{3L^2x}{64} \quad 0 \leq x \leq L/4 \quad (A13)$$

For the load at a point $L/4$, Equation (A13) becomes

$$w = \frac{PL}{8bkA_{55}} + \frac{D_{11}^{-1} PL^3}{96b} \quad (A14)$$

Equation (A14) now gives the deflection with the shear distortion included.

Appendix B

Physical Description of Specimens

1. Interlaminar Normal Stress Verification Specimen

Ply Geometry: $(0^\circ, \pm 45^\circ, 90^\circ)_s$ 8 plies of graphite/epoxy material.

Dimensions: Width = 0.47 in.

Height = 0.11 in.

Length = 3.0 in.

Material Properties: $E_L = 20 \times 10^6$ psi $G_{LT} = 0.8 \times 10^6$ psi

$E_T = 1.3 \times 10^6$ psi $\nu_{LT} = 0.25$

2. Thermal Edge Effect Stress Distribution Specimen

Ply Geometries: $(0^\circ, 90^\circ)_s$

$(90^\circ, 0^\circ)_s$ 4 plies of graphite/epoxy material

$(\pm 45^\circ)_s$

Dimensions: Width = 1.6 in.

Height = 0.4 in.

Length = 4.0 in.

Material Properties: $E_L = 20 \times 10^6$ psi $\nu_{LT} = 0.21$

$E_T = 2.1 \times 10^6$ psi $\alpha_L = 0.2 \times 10^{-6}/^\circ\text{F}$

$G_{LT} = 0.85 \times 10^6$ psi $\alpha_T = 16.0 \times 10^{-6}/^\circ\text{F}$

3. Hybrid Addition Effect Specimen

Ply Geometry: $(0^\circ, \pm 45^\circ, 90^\circ)_s$ 8 plies of graphite/epoxy and
graphite/glass/epoxy material

Dimensions: Width = 1.6 in.

Height = 0.4 in.

Length = 4.0 in.

Material Properties:

Graphite/Epoxy Material

$$\begin{array}{lll} E_L = 18.2 \times 10^6 \text{ psi} & \nu_{LT} = 0.21 & x = 1.5 \times 10^5 \text{ psi} \\ E_T = 1.77 \times 10^6 \text{ psi} & \alpha_L = 0.7 \times 10^{-6} / ^\circ\text{F} & y = 6.0 \times 10^3 \text{ psi} \\ G_{LT} = 0.85 \times 10^6 \text{ psi} & \alpha_T = 16.0 \times 10^{-6} / ^\circ\text{F} & s = 1.0 \times 10^4 \text{ psi} \end{array}$$

80-20 Graphite/Glass Hybrid Material

$$\begin{array}{lll} E_L = 15.6 \times 10^6 \text{ psi} & \nu_{LT} = 0.20 & x = 1.9 \times 10^5 \text{ psi} \\ E_T = 1.59 \times 10^6 \text{ psi} & \alpha_L = 0.86 \times 10^{-6} / ^\circ\text{F} & y = 9.8 \times 10^3 \text{ psi} \\ G_{LT} = 0.78 \times 10^6 \text{ psi} & \alpha_T = 15.08 \times 10^{-6} / ^\circ\text{F} & s = 1.59 \times 10^4 \text{ psi} \end{array}$$

4. Hybrid Flexure Analytical Specimen

Ply Geometry: $(\pm 45^\circ, 0^\circ, 0^\circ, \pm 35^\circ)_s$ 12 plies of glass/epoxy and graphite/glass/epoxy material

Dimensions: Width = 0.48 in.

Height = 0.12 in.

Length = 4.0 in.

Material Properties:

Glass/Epoxy Material

$$\begin{array}{lll} E_L = 6.3 \times 10^6 \text{ psi} & \nu_{LT} = 0.3 & x = 1.5 \times 10^5 \text{ psi} \\ E_T = 0.7 \times 10^6 \text{ psi} & \alpha_L = 3.5 \times 10^{-6} / ^\circ\text{F} & y = 4.0 \times 10^3 \text{ psi} \\ G_{LT} = 0.7 \times 10^6 \text{ psi} & \alpha_T = 11.4 \times 10^{-6} / ^\circ\text{F} & s = 6.0 \times 10^3 \text{ psi} \end{array}$$

80-20 Graphite/Glass Material

$$\begin{array}{lll} E_L = 15.6 \times 10^6 \text{ psi} & \nu_{LT} = 0.2 & x = 1.9 \times 10^5 \text{ psi} \\ E_T = 1.5 \times 10^6 \text{ psi} & \alpha_L = 0.86 \times 10^{-6} / ^\circ\text{F} & y = 9.8 \times 10^3 \text{ psi} \\ G_{LT} = 0.78 \times 10^6 \text{ psi} & \alpha_T = 15.08 \times 10^{-6} / ^\circ\text{F} & s = 1.59 \times 10^4 \text{ psi} \end{array}$$

5. 48 Ply Hybrid Specimens

Ply Geometry: 48 plies of materials described in specimen #4.

Specimens are symmetric about mid plane.

1 - $+45^{\circ}$	7 - 0°	13 - 0°	19 - $+35^{\circ}$
2 - -45°	8 - $+35^{\circ}$	14 - -35°	20 - $+35^{\circ}$
3 - $+45^{\circ}$	9 - 0°	15 - 0°	21 - $+35^{\circ}$
4 - -45°	10 - -35°	16 - 0°	22 - $+35^{\circ}$
5 - -35°	11 - 0°	17 - 0°	23 - 0°
6 - -35°	12 - $+35^{\circ}$	18 - 0°	24 - 0°

In specimen #1, plies 1, 2, 3, 4, 7, 9, 11 and 13 are glass/epoxy material. In specimen #2 only plies 1, 2, 3 and 4 are glass/epoxy. All other plies are 80-20 hybrid material.

Dimensions: Width = 0.4949 in.

Height = 0.2491 in. Average

Length = 4 in.

Material Properties: Same as those described in specimen #4.

6. A standard straight sided coupon of 1/2 in. width was employed for the tensile tests. End tabs were attached so that they overlapped the width of the specimen. These tabs insure distribution of the clamp compressive loads. Tests were performed on an Instron testing machine. The flexure specimens were 1/2 in. wide and 4 in. in length. A standard four-point load test was used with 16:1 span-to-depth ratio. Deflections were measured by the chart drive method. Crosshead loads were applied at L/4 and 3L/4 points. Measured crosshead deflection was the quarter point deflection.

Vita


George Brooks was born on 9 June 1944 in DeQueen, Arkansas. He graduated from DeQueen High School in 1962. He graduated from Louisiana Polytechnic Institute in 1967 with a Bachelor of Science Degree in Mechanical Engineering. He completed undergraduate pilot training in 1968 and spent the next eight years in operational squadrons flying the F-102, O-2A, and F-106 aircraft. In June 1976 he enrolled in the Air Force Institute of Technology in the Graduate Aeronautical Structures Engineering Program.

Permanent address: Rt. 1, Box 779
DeQueen, Arkansas 71832

REPORT DOCUMENTATION PAGE		READ INSTRUCTIONS BEFORE COMPLETING FORM
1. REPORT NUMBER 14 AFIT/GAE/AA/77D-2 ✓	2. GOVT ACCESSION NO.	3. RECIPIENT'S CATALOG NUMBER
4. TITLE (and Subtitle) 6 GENERAL STUDY OF HYBRID COMPOSITE LAMINATES.	5. TYPE OF REPORT & PERIOD COVERED 9 Master's thesis, MS THESIS ✓	6. PERFORMING ORG. REPORT NUMBER
7. AUTHOR(s) 10 George D./Brooks Captain USAF	8. CONTRACT OR GRANT NUMBER(s)	10. PROGRAM ELEMENT, PROJECT, TASK AREA & WORK UNIT NUMBERS
9. PERFORMING ORGANIZATION NAME AND ADDRESS Air Force Institute of Technology (AFIT/ENA) Wright-Patterson AFB, Ohio 45433	11. CONTROLLING OFFICE NAME AND ADDRESS Air Force Materials Laboratory (AFML) Wright-Patterson AFB, Ohio 45433	12. REPORT DATE 11 Dec 1977 12 35 p.
14. MONITORING AGENCY NAME & ADDRESS (if different from Controlling Office)	15. SECURITY CLASS. (of this report) UNCLAS	15a. DECLASSIFICATION/DOWNGRADING SCHEDULE
16. DISTRIBUTION STATEMENT (of this Report) Approved for public release; distribution unlimited.		
17. DISTRIBUTION STATEMENT (of the abstract entered in Block 20, if different from Report)		
18. SUPPLEMENTARY NOTES Approved for public release; IAW AFR 190-17 JERREL F. GUESS, Captain, USAF Director of Information		
19. KEY WORDS (Continue on reverse side if necessary and identify by block number) Hybrid laminates Hybrid composite laminates Composite laminates 012 225		
20. ABSTRACT (Continue on reverse side if necessary and identify by block number) This thesis is a general study of hybrid composite laminates that includes application of a three dimensional stress analysis approximation technique based on equilibrium considerations and free edge effects. Thermal residual stresses and effects of replacing lamina in a composite laminate with lamina composed of hybrid material were investigated. Two types of 48 ply hybrid composite laminates were tested under tensile and flexure loading. Results achieved experimentally for the moduli of elasticity were compared with values predicted by laminated plate theory and laminated beam theory. Thermal residual		

UNCLASSIFIED

SECURITY CLASSIFICATION OF THIS PAGE(When Data Entered)

20. stresses proved to be significant and worthy of due consideration in stress analysis of test specimens. Hybridization, as studied, appeared to have little effect on the overall properties of a laminate. Hybrid composite laminates obey classical laminate theory and can, in certain ply configurations, develop considerable free edge effect stresses.
- 

UNCLASSIFIED

SECURITY CLASSIFICATION OF THIS PAGE(When Data Entered)